Received: 17 August 2023 | Accepted: 15 February 2024

DOI: 10.1111/ene.16266

european journal of neurology
the official journal of the european academy of neurology

ORIGINAL ARTICLE

Distinct neural signatures of pulvinar in *C9orf72* amyotrophic lateral sclerosis mutation carriers and noncarriers

Anna Nigri[1] | Mario Stanziano[1,2] | Davide Fedeli[1] | Umberto Manera[2,3] | Stefania Ferraro[1,4] | Jean Paul Medina Carrion[1] | Sara Palermo[1] | Laura Lequio[5] | Federica Denegri[5] | Federica Agosta[6,7,8] | Edoardo Gioele Spinelli[6,7,9] | Massimo Filippi[6,7,8,9,10] | Marina Grisoli[1] | Maria Consuelo Valentini[5] | Filippo De Mattei[2,3] | Antonio Canosa[2,3] | Andrea Calvo[2,3] | Adriano Chiò[2,3,11] | Maria Grazia Bruzzone[1] | Cristina Moglia[2,3]

[1]Neuroradiology Unit, Fondazione IRCCS Istituto Neurologico Carlo Besta, Milan, Italy

[2]ALS Centre, "Rita Levi Montalcini" Department of Neuroscience, University of Turin, Turin, Italy

[3]Azienda Ospedaliero-Universitaria Città della Salute e della Scienza di Torino, SC Neurologia 1U, Turin, Italy

[4]School of Life Science and Technology, MOE Key Laboratory for Neuroinformation, University of Electronic Science and Technology of China, Chengdu, China

[5]Neuroradiology Unit, CTO Hospital, AOU Città della Salute e della Scienza di Torino, Turin, Italy

[6]Neuroimaging Research Unit, Division of Neuroscience, IRCCS San Raffaele Scientific Institute, Milan, Italy

[7]Neurology Unit, IRCCS San Raffaele Scientific Institute, Milan, Italy

[8]Vita-Salute San Raffaele University, Milan, Italy

[9]Neurorehabilitation Unit, IRCCS San Raffaele Scientific Institute, Milan, Italy

[10]Neurophysiology Service, IRCCS San Raffaele Scientific Institute, Milan, Italy

[11]Institute of Cognitive Sciences and Technologies, National Council of Research, Rome, Italy

Correspondence
Mario Stanziano, ALS Centre, Department of Neuroscience "Rita Levi Montalcini," University of Turin, via Cherasco 15, 10126 Torino, Italy.
Email: mario.stanziano@istituto-besta.it

Funding information
Ministero dell'Università e della Ricerca, Grant/Award Number: 2017SNW5MB; European Commission's Health Seventh Framework Programme, Grant/Award Number: FP7/2007-2013 and 259867; Ministero della Salute, Grant/Award Number: GR-2019-12371291, RF-2016-02362405 and RRC

Abstract

Background and purpose: Thalamic alterations have been reported as a major feature in presymptomatic and symptomatic patients carrying the *C9orf72* mutation across the frontotemporal dementia–amyotrophic lateral sclerosis (ALS) spectrum. Specifically, the pulvinar, a high-order thalamic nucleus and timekeeper for large-scale cortical networks, has been hypothesized to be involved in *C9orf72*-related neurodegenerative diseases. We investigated whether pulvinar volume can be useful for differential diagnosis in ALS *C9orf72* mutation carriers and noncarriers and how underlying functional connectivity changes affect this region.

Methods: We studied 19 ALS *C9orf72* mutation carriers (*ALSC9+*) accurately matched with wild-type ALS (*ALSC9−*) and ALS mimic (*ALSmimic*) patients using structural and resting-state functional magnetic resonance imaging data. Pulvinar volume was computed using automatic segmentation. Seed-to-voxel functional connectivity analyses were performed using seeds from a pulvinar functional parcellation.

Maria Grazia Bruzzone and Cristina Moglia equally contributed to this article.

Results: Pulvinar structural integrity had high discriminative values for *ALSC9+* patients compared to *ALSmimic* (area under the curve [AUC] = 0.86) and *ALSC9−* (AUC = 0.77) patients, yielding a volume cutpoint of approximately 0.23%. Compared to *ALSmimic*, *ALSC9−* showed increased anterior, inferior, and lateral pulvinar connections with bilateral occipital–temporal–parietal regions, whereas *ALSC9+* showed no differences. *ALSC9+* patients when compared to *ALSC9−* patients showed reduced pulvinar–occipital connectivity for anterior and inferior pulvinar seeds.

Conclusions: Pulvinar volume could be a differential biomarker closely related to the *C9orf72* mutation. A pulvinar–cortical circuit dysfunction might play a critical role in disease progression and development, in both the genetic phenotype and ALS wild-type patients.

KEYWORDS
amyotrophic lateral sclerosis, *C9orf72* mutation, fMRI, MRI, pulvinar

INTRODUCTION

Amyotrophic lateral sclerosis (ALS) is a progressive neurodegenerative disease associated with the impairment of lower and upper motor neurons and some associated pathways [1]. ALS is a multifaceted disease, with different clinical and neuropsychological symptoms. Hexanucleotide GGGGCC repeat expansion in the *C9orf72* gene is the most frequent genetic cause of ALS and frontotemporal dementia (FTD) [2, 3] and occurs in 20%–40% of familiar and 3%–8% of sporadic cases [4, 5]. *C9orf72* mutation carriers are associated with more severe forms of ALS that increase the disease heterogeneity. When compared with non-mutated carriers, patients carrying the C9orf72 hexanucleotide repeat expansion showed an earlier disease onset [6–8], higher odds of bulbar onset [6, 9], and a higher disease progression, which also determines a shorter survival [6–8].

Neuroimaging studies reported thalamic alterations as a main feature of presymptomatic and symptomatic ALS and FTD patients carrying the *C9orf72* mutation [10–12]. In particular, a specific volume decrease has been observed in the pulvinar nucleus (i.e., the largest and most posterior thalamic nucleus) in presymptomatic and FTD *C9orf72* mutation carriers when compared with healthy controls [13–16]. A similar trend was also observed in two ALS patients affected by the *C9orf72* mutation [15], supporting the hypothesis that a specific involvement of this region in *C9orf72*-related neurodegenerative diseases may occur across the FTD–ALS spectrum [14, 15, 17].

The pulvinar is a higher order nucleus of the thalamus implicated in various functions such as attention, emotion and social recognition, voluntary actions, and saccades [18, 19]. It is considered a timekeeper for large-scale cortical networks [20], supporting a central role in the coordination of cortico-subcortical processes [19, 21].

Previous studies reported that pulvinar–cortical feedforward and feedback pathways increased the computational capabilities of otherwise isolated cognitive cortical circuits, allowing for additional control and flexibility [20, 22]. Interestingly, the pulvinar itself has been indicated to be functionally heterogeneous [19, 21]. A recent study, using a data-driven method, identified five distinct functional subregions of the pulvinar to which different pulvinar–cortical connectivity fingerprints and cognitive domains are associated [21]. This partitioning largely overlaps with the anatomical classification based on cytoarchitectonic areas [21].

To elucidate the involvement of the pulvinar nucleus in the pathophysiology of *C9orf72* mutation-driven ALS, 19 ALS *C9orf72* mutation carriers were matched with wild-type ALS and ALS mimic patients. The purpose of this study is twofold: (i) to assess whether the structural integrity of the pulvinar discriminates between ALS *C9orf72* mutation carriers and non-carriers for a differential diagnosis; and (ii) to evaluate the underlying changes in pulvinar functional connectivity among patients, according to its known distinct functional profiles. We suggest a distinct role of the pulvinar region in the anatomo–functional pathological profile of *C9orf72*-mediated ALS versus non-carriers. If this relationship is proven to be significant, structural and functional features of the pulvinar nucleus could be used as a biomarker of *C9orf72* mutation carriers.

MATERIALS AND METHODS

Participants

Thirty-eight patients diagnosed with ALS (El Escorial Revised Criteria) [23] and 19 ALS mimic patients (*ALSmimic*) were included in the study (enrolment 2011–2019). The retrospective study was carried out in accordance with the Declaration of Helsinki, and it was approved by the Ethical Committee of the Azienda Ospedaliero-Universitaria Citt. della Salute of Turin (Protocol N.0021674–24/02/2022). All participants gave their written consent. *ALSmimic* patients, without primary neurodegenerative diseases, were affected by clinical conditions with features resembling those of ALS: cervical spondylotic myelopathy ($n = 3$), myasthenia gravis ($n = 9$), monomelic amyotrophy (Hirayama disease; $n = 1$), and peripheral motor neuropathy ($n = 6$).

All *ALSmimic* patients were initially recruited as suspected or possible ALS cases and were later diagnosed as mimics. Comorbidity of severe neurological or psychiatric conditions was considered an exclusion criteria. Among ALS patients, 19 ALS patients carrying *C9orf72* expansion (*ALSC9+*) were paired with 19 wild-type patients (*ALSC9−*). *ALSC9+*, *ALSC9−*, and *ALSmimic* were carefully matched for age (±5 years) and sex assigned at birth (female:female, male:male), and *ALSC9+* and *ALSC9−* patients were also paired for Amyotrophic Lateral Sclerosis Functional Rating Scale - Revised (ALSFRS-R) total score at the time of magnetic resonance imaging (MRI; ±5 points) and disease duration from the onset (±3 months) using a one-by-one pairing technique, as described in previous studies [24, 25]. All patients included had no mutation in *SOD1*, *TARDBP*, and *FUS* genes. Number of body regions involved was assessed using King's staging system [26]. Exclusion criteria for all participants were any major psychiatric or other neurological illnesses, causes of focal or diffuse brain damage, including lacunae, and extensive cerebrovascular disorders on routine MRI. Demographic and clinical data are reported in Table 1.

MRI acquisition

MRI acquisition was performed with a 1.5-T General Electric Signa HD-XT scanner equipped with an eight-channel head coil at the Neuroradiology Unit, AOU Città della Salute e della Scienza di Torino. For each participant, a three-dimensional T1-weighted anatomical image (repetition time = 11.85 ms, echo time = 4.9 ms, flip angle = 12°, matrix size = 512 × 512, number of axial slices = 120, voxel size = 0.47 × 0.47 × 1 mm^3, whole-brain coverage) and resting-state functional magnetic resonance (fMRI) images (echo planar imaging sequence: repetition time = 2250 ms, echo time = 50 ms, flip angle = 90°, matrix size = 64 × 64, voxel size = 3.28 × 3.28 × 5 mm^3, interslice gap = 1 mm, 25 axial slices, number of volumes = 585) were acquired.

Structural MRI data analysis

T1-weighted anatomical images were segmented with FreeSurfer (v7, http://surfer.nmr.mgh.harvard.edu/) [27]. After the "recon-all" pipeline, the thalamic nuclei segmentation module was applied [28].

Estimated total intracranial volume, thalamus, and pulvinar subnuclei volume were extracted for each participant using the same tool [28]. Pulvinar and thalamus volumes were expressed as a percentage of total intracranial volume.

Resting-state fMRI data analysis

The CONN toolbox (version 20.b, Matlab R2023a) [29] implemented in SPM12 was used to perform resting-state fMRI images data analyses. CONN's "default_MNI" preprocessing pipeline was used. The following processing steps were performed: realignment to the first functional image and unwarping slice-timing correction (slice order = interleaved, bottom-up); outlier identification with the Artifact Rejection Toolbox (framewise displacement > 1.1 mm; global blood oxigenation level dependent signal changes > 5); direct segmentation in gray matter, white matter, and cerebrospinal fluid tissue classes; registration and normalization of resting-state fMRI images and T1-weighted images into standard Montreal Neurological Institute (MNI) space [30]; resting-state fMRI image data resampling to 2-mm isotropic voxels, and T1-weighted image resampling to 1-mm isotropic voxels; smoothing with a full width at half maximum 6 × 6 × 6-mm [3] Gaussian kernel. Data denoising was performed with the anatomical component-based noise correction (aCompCor) to extract mean physiological noise signals from white matter and cerebrospinal fluid maps [31]. For each participant, realignment, outlier volumes scrubbing parameters, physiological noise signals from white matter and cerebrospinal fluid, and "effect of rest" (initial magnetization transient effects) were entered as nuisance covariates in the first-level analysis [32]. Subsequently, a 0.008–0.1-Hz bandpass filter was applied to the time series to remove low-frequency drifts and high-frequency noise.

Statistical analyses

To test between-group differences (i.e., *ALSC9+*, *ALSC9−*, and *ALSmimic*) for demographic and clinical variables, two-sample independent *t*-test/one-way analysis of variance (ANOVA; for age, disease duration, survival, ALSFRS-R score, ALSFRS-R slope, King's staging) and chi-squared (for sex assigned at birth and onset type) tests were used, after determining the normality of data distribution with the Kolmogorov–Smirnov test. All results were considered significant at $p \leq 0.05$ and adjusted for multiple comparisons.

The interquartile range method was used to identify outliers for each group in volumes of pulvinar region; a measure is declared an outlier if it is 1.5 times higher or 1.5 times lower than its interquartile range. A Pearson correlation was applied to assess significant associations between the pulvinar volume in each group and the clinical variables (age, disease duration, and ALSFRS-R score).

Using a set of logistic regression models, we investigated the relationship between the volume of the pulvinar (predictor variable) and the diagnosis (response variable). To this end, we determined whether this measure could discriminate between (i) the diagnosis of *ALSC9+* and *ALSmimic*, (ii) the diagnosis of *ALSC9−* and *ALSmimic*, and (iii) the diagnosis of *ALSC9+* and *ALSC9−*. Preliminary analyses were performed to check for multicollinearity between age, sex assigned at birth, and pulvinar volume. Covariates were included if the variance inflation factor was <10. For each model, the odds ratios (ORs) and corresponding *p*-values, after Holm–Bonferroni correction for multiple comparisons, were calculated. The area under the receiver operating characteristic curve (AUC) was used to measure the diagnostic discrimination accuracy of each multiple logistic regression model, and the optimal volume cutpoint value was computed. We

TABLE 1 Demographic and clinical characteristics of patients.

Characteristic	*ALSC9+*, $n = 19$	*ALSC9−*, $n = 19$	*ALSmimic*, $n = 19$	p[a]
Male/female ratio	10/9	10/9	10/9	1
Bulbar/spinal onset	13/6	11/8	-	0.68
	Median (IQR)	Median (IQR)		p[b]
Age, years	55.50 (51.15–69.70)	59.50 (53.45–66.05)	60.00 (53.00–69.00)	0.99
ALSFRS-R score	43.00 (38.50–45.00)	43.00 (37.50–45.00)	-	0.95
Disease duration, months	11.0 (8.00–14.50)	11.0 (9.00–13.50)	-	0.94
Overall survival, years	2.57 (2.19–3.17)	2.70 (2.13–3.40) [4 alive]	-	0.91
Disease progression, ΔALSFRS-R	0.53 (0.28–0.78)	0.56 (0.27–0.91)	-	0.67
Number of body regions involved	2.57 (2.19–3.17)	2.00 (1.00–2.00)	-	0.74
Weight loss, kg/month	0 (0–0.35)	0.23 (0.12–0.89)	-	0.09
FVC, %	91 (86–104)	91 (84–104)	-	1
	n	*n*		
Onset of symptoms				
Motor	18	18	-	1
Cognitive	1	1	-	
Cognitive classification				
Normal cognition	7	13	-	0.28
ALSbi	1	2	-	
ALSci	2	1	-	
ALScbi	1	0	-	
ALS–FTD	5	1	-	
Unknown	3	2	-	
Psychiatric symptoms[c]				
No	16	15	-	1
Yes	1 psychosis 2 depression	2 anxiety and depression 2 depression	-	

Abbreviations: ALS, amyotrophic lateral sclerosis; ALSbi, behavioural impairment; ALSci, cognitive impairment; ALScbi, cognitive and behavioural impairment; *ALSC9−*, ALS patients not carrying *C9orf72* expansion; *ALSC9+*, ALS patients carrying *C9orf72* expansion; ALSFRS-R, Amyotrophic Lateral Sclerosis Functional Rating Scale–Revised; *ALSmimic*, ALS mimic patients; FTD, frontotemporal dementia; FVC, forced vital capacity; IQR, interquartile range.

[a]Results for chi-square test among *ALSC9+*, *ALSC9−*, and *ALSmimic*.

[b]Results for two-sample independent *t*-test between *ALSC9+* and *ALSC9−* and for one-way analysis of variance among *ALSC9+*, *ALSC9−*, and *ALSmimic*.

[c]All patients with psychiatric symptoms were undergoing pharmacological treatment, except for one ALS patient with depression. Weight loss was calculated as the ratio of weight kilograms lost and months elapsed between the onset and diagnosis of the disease.

estimated the interquartile range around the volume cutpoint using a bootstrap test (1000 iterations).

Analyses were performed with SciPy [33] and Statsmodels [34] running on Python3, and the Cutpointr package [35] implemented in R.

Seed-to-voxel resting-state functional connectivity

To identify functional alterations of the pulvinar region among groups, we performed a seed-to-voxel functional connectivity analysis. The pulvinar nucleus functional parcellation by Guedj and Vuilleumier [21] was used to define five bilateral seeds: dorsomedial, ventromedial, lateral, anterior, and inferior pulvinar. The authors used a data-driven method to partition the pulvinar into distinct subregions according to their functional connectivity profiles with the rest of the brain. This parcellation allows us to assess functional changes in patients taking into account the heterogeneity of the pulvinar's functional organization [19, 21].

At the first-level analyses, whole-brain bivariate correlations were performed between the time series of each bilateral seed (i.e., average signal across all voxels within the left hemispheric and right hemispheric seeds) and the time series of all the other brain voxels. Voxelwise correlation coefficients were subsequently

R- to *Z*-score converted. Second-level general linear model analyses were performed to compare the functional connectivity profiles of each bilateral pulvinar seed among groups (*ALSC9+*, *ALSC9−*, and *ALSmimic*). Age, sex assigned at birth, and whole thalamus volume were included as nuisance covariates. The following contrasts were investigated: (i) *ALSC9−* versus *ALSmimic*, (ii) *ALSC9+* versus *ALSmimic*, and (iii) *ALSC9+* versus *ALSC9−*. For all the contrasts, the significance threshold was kept at CONN 20b's default settings using both voxel and cluster thresholds: voxel *p*-uncorrected <0.005 and cluster false discovery rate-corrected *p* for multiple comparisons <0.05.

RESULTS

Structural pulvinar assessment

No significant difference in demographic and clinical variables were found between groups (Table 1).

Only one outlier was identified in the pulvinar volume of the *ALSC9+* patient group, exceeding its interquartile range by 1.5 times. Age was significantly correlated with pulvinar volume in the *ALSC9−* and *ALSmimic* patients ($R=-0.66$, $p=0.002$; $R=-0.58$, $p=0.009$, respectively) but not in the *ALSC9+* group ($R=-0.26$, $p=0.3$). No significant correlations were observed between the pulvinar volume and the other variables (i.e., disease duration and ALSFRS-R score).

Logistic regression models—no covariates were included (variance inflation factor >10)—showed that the decrease in volume of the bilateral pulvinar ($p=0.003$, OR$=0.57$, 95% confidence interval [CI] $=0.40–0.82$) discriminated *ALSC9+* patients from *ALSmimic* subjects. A volume decrease of the same region was able to successfully discriminate *ALSC9+* from *ALSC9−* ($p=0.009$, OR$=0.49$, 95% CI$=0.49–0.90$). Meanwhile, no significant results were found in the logistic regression on pulvinar volume between *ALSC9−* and *ALSmimic* ($p=0.147$). The AUC diagnostic accuracy of pulvinar was 0.86 (95% CI$=0.73–0.96$) with a volume cutpoint of 0.23% (95% CI$=0.22\%–0.26\%$) between *ALSC9+* patients and *ALSmimic* subjects and 0.77 (95% CI$=0.59–0.91$) with a volume cutpoint of 0.23% (95% CI$=0.21\%–0.25\%$) between *ALSC9+* patients and *ALSC9−* subjects (Figure 1).

Seed-to-voxel resting-state functional connectivity: *ALSC9−* versus *ALSmimic*

Compared to *ALSmimic*, *ALSC9−* patients showed significant functional connectivity changes of the anterior, dorsomedial, inferior, and lateral pulvinar seeds with posterior cortical regions (Figure 2a,

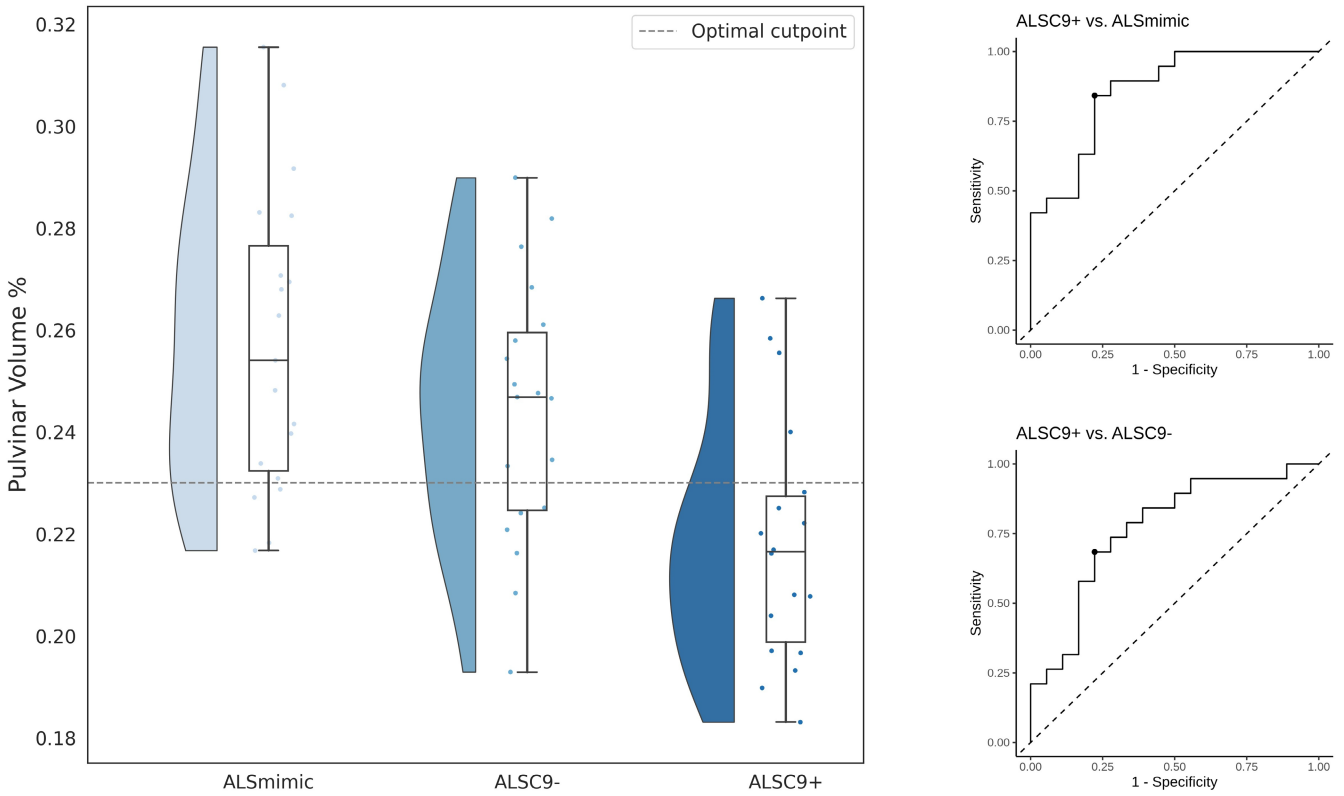

FIGURE 1 Diagnostic accuracy of pulvinar volume. On the left, violin plots and boxplots depict the pulvinar volume distributions according to group classification (amyotrophic lateral sclerosis [ALS] mimic patients [*ALSmimic*], ALS patients not carrying *C9orf72* expansion [*ALSC9−*], ALS patients carrying *C9orf72* expansion [*ALSC9+*]). The dashed line indicates the optimal pulvinar volume cutpoint identified (0.23%). On the right, receiver operating curves indicate the sensitivity and specificity of pulvinar volume in differentiating *ALSC9+* versus *ALSmimic* (0.86) and *ALSC9+* versus *ALSC9−* (0.77) patient groups.

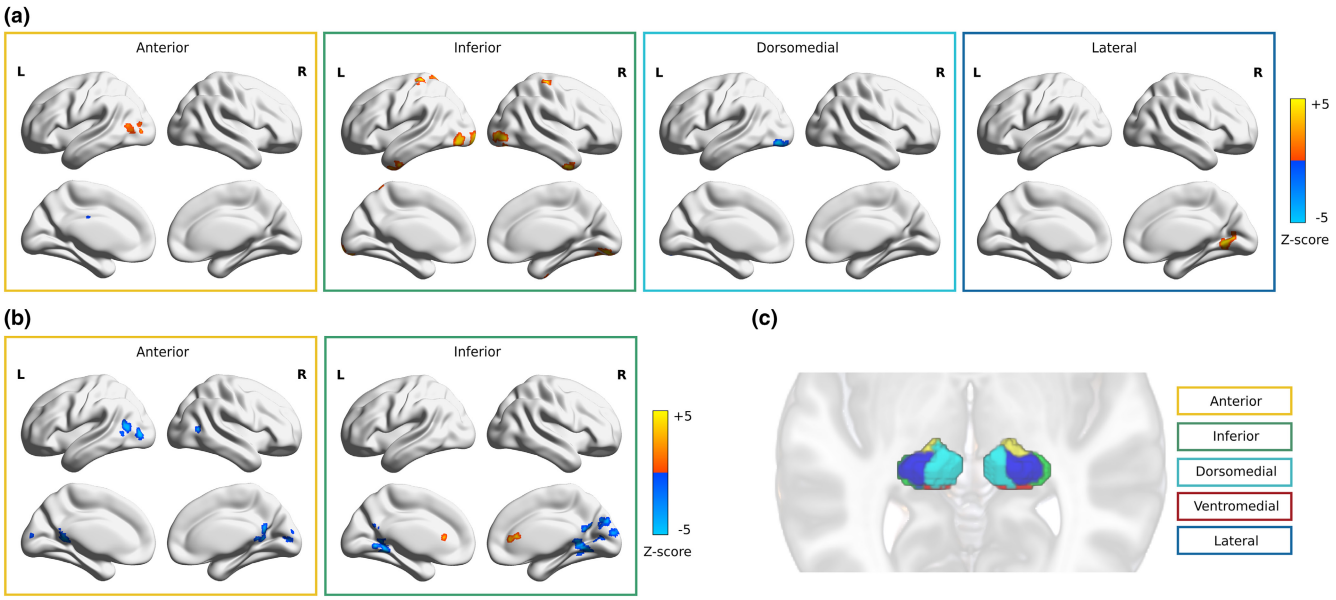

FIGURE 2 Pulvinar functional connectivity. Significant functional connectivity changes of the anterior, dorsomedial, inferior, and/or lateral pulvinar seed in *ALSC9−* compared to *ALSmimic* patients (a) and in *ALSC9+* compared to *ALSC9−* patients (b). (c) Pulvinar nucleus functional parcellation by Guedj and Vuilleumier [21]. L, left; R, right.

Table S1). The most extensive functional alterations in *ALSC9−* patients compared to *ALSmimics* were reported for the bilateral inferior pulvinar seed, which showed increased functional connectivity in the bilateral lateral–occipital, postcentral, and anterior inferior temporal regions. The bilateral anterior seed showed an increase in functional connectivity confined to the left lateral occipital cortex, whereas the bilateral lateral seed showed an increase in functional connectivity in the right lingual gyrus. On the other hand, the bilateral dorsomedial seed showed a decrease in functional connectivity in the left lateral occipital region.

Seed-to-voxel resting-state functional connectivity: *ALSC9+* versus *ALSmimic*

No significant functional connectivity changes between *ALSC9+* and *ALSmimic* were identified in each pulvinar seed.

Seed-to-voxel resting-state functional connectivity: *ALSC9+* versus *ALSC9−*

Significant pulvinar–occipital functional connectivity changes were reported for anterior and inferior pulvinar regions in *ALSC9+* patients when compared to *ALSC9−* (Figure 2b, Table S1). The bilateral anterior pulvinar seed showed a decrease of functional connectivity with the bilateral lateral occipital cortex, left precuneus, and right intracalcarine cortex in *ALSC9+* patients. The inferior pulvinar seed exhibited an increase of functional connectivity with the right anterior cingulate gyrus in *ALSC9+* patients, and a decreased functional connectivity with the right cuneus and precuneus, and bilateral lingual gyri.

DISCUSSION

In this work, we observed that the pulvinar region has a distinct neurofunctional pathological profile in *C9orf72*-mediated and non-mediated ALS. Structural data showed that a decrease in whole pulvinar volume could represent a potential marker for differential diagnosis. Based on pulvinar atrophy, we were able to discriminate mutation carriers from both *ALSmimic* (AUC = 0.86, cutpoint = 0.23%) and wild-type ALS patients with similar disease burden (AUC = 0.77, cutpoint = 0.23%). Furthermore, we identified between-group functional connectivity alterations of pulvinar subregions. Notably, *ALSC9−* patients, compared to *ALSmimic*, showed mainly increased functional connectivity in inferior, anterior, lateral, and dorsomedial pulvinar with posterior areas, including bilateral occipital–temporal–parietal regions, whereas *ALSC9+* showed no significant functional abnormalities. *ALSC9+* patients, when compared to *ALSC9−* patients, presented a decreased occipital functional connectivity for anterior and inferior pulvinar subregions.

Previous literature on the ALS–FTD spectrum mediated by the *C9orf72* mutation and the specific clinical features of these patients largely supports an involvement of the pulvinar in the disease in both the presymptomatic [13] and symptomatic phases [14, 15].

Remarkably, our structural data confirmed an impaired bilateral pulvinar also in *C9orf72*-carrying ALS patients, in addition to the findings reported in patients with FTD [14, 15]. The volume of this region has high diagnostic accuracy in patients who carry the mutation, not only when compared to ALS mimics (AUC = 0.86, cutpoint = 0.23), but also when compared to wild-type ALS patients (AUC = 0.77, cutpoint = 0.23). Previous studies differentiating *C9orf72* mutation

carriers from sporadic FTD and/or ALS patients reported an AUC ranging from 0.68 to 0.82 when considering the whole thalamus volume [36, 37] and 0.88 for a combination of the volume of the prefrontal and the laterality index of the thalamic occipital subregion [36]. Together, these observations suggest that MRI volumetry of the thalamus, especially the pulvinar, has a high predictive value for identifying *C9orf72* mutation carriers. Moreover, although the specific involvement of the pulvinar nucleus is reported in patients with psychiatric disorders [38, 39], we point out that our ALS patients affected by the gene mutation do not appear to exhibit more psychiatric symptoms than non-carriers.

With respect to the resting-state functional connectivity, we observed alterations in both mutation-carrying and non-carrying patients.

In *ALSC9*− patients compared to *ALSmimic* patients, all the functional subnuclei of the pulvinar, except for the ventromedial, mainly showed increased functional connectivity with the posterior cortical regions. Altered cortical areas included mainly the occipital, fusiform, and lingual regions, followed by the postcentral gyri and anterior temporal region.

Increased or decreased resting-state connectivity in posterior regions, including occipital and temporal lobes, has been reported in ALS patients in several studies [37, 40–42] and associated with altered functional connectivity of the thalamus [40, 41, 43]. Progressive decreases in functional connectivity have been identified in sensorimotor, thalamic, and visual networks also longitudinally and with ALSFRS-R decline [44]. This increase in functional connectivity could be a compensatory phenomenon in ALS patients. This phenomenon may precede the structural alteration and/or decrease of functional connectivity that might appear in the later stages of the pathology due to neurodegeneration [1, 40, 41, 44]. This suggests that functional pulvinar abnormalities may emerge in the early stages of ALS and contribute to cognitive and behavioral changes with the disease progression [45].

On the other hand, *ALSC9*+ patients, in the presence of marked structural atrophy, showed a functional connectivity decrease in occipital region and an increase in anterior cingulate for the anterior and inferior pulvinar compared to *ALSC9*− patients, but not *ALSmimic* patients. The anterior seed is mainly related to motor processes, whereas the inferior seed is related to cognitive functions, especially face recognition and memory [21]. Patients with *C9orf72*-related FTD showed similar reduced functional connectivity changes in the anterior pulvinar functional seed—referred to as medial pulvinar in previous studies (MNI coordinates fall within our anterior pulvinar seed)—compared to non-mutated carriers [17]. In agreement with a previous study, these alterations could be the result of a slight reduction in connectivity in *ALSC9*+ and an enhancement in *ALSC9*− (compared to *ALSmimic* or healthy controls), although not detectable in *ALSC9*+ [17].

Moreover, we observed in our age-matched cohort that the pulvinar volume in *ALSmimic* and *ALSC9*− patients decreased as their age increased, whereas this association was not shown in *ALSC9*+ patients. Hence, structural abnormalities in the pulvinar remained consistently reduced throughout the age span examined, without worsening with age in mutation carriers. These trends in structural and functional alterations reinforce the hypothesis that the structural alteration of the pulvinar in C9orf carriers could be linked to the neurodevelopmental profile [46], which might lead a functional adaptation over time, even if reduced in some occipital–parietal regions, as we reported. This hypothesis is corroborated by the longitudinal observation of presymptomatic *C9orf72* carriers in which the decrease of thalamic functional connectivity (MNI coordinates of thalamic seeds fall within the anterior seed of pulvinar) was stable over time [47]. It has been suggested that maintaining the topography of functional networks facilitates cognitive resilience in the face of ongoing structural changes in presymptomatic patients [16, 48, 49]. When patients become symptomatic, the integrity of these functional networks declines [48].

In addition to its strengths—the sample size and matching for the disease burden of patients—this study has some limitations. First, it was not possible to include a standard healthy control group. However, the inclusion of *ALSmimic* provided us with a unique opportunity to highlight important traits of *C9orf72* carrier and non-carrier ALS patients as compared to patients whose clinical presentation may resemble those of ALS patients at the outset. One of the manifold goals of reliable markers of ALS-related alterations is to allow early diagnosis with high sensitivity and specificity, notably in the differential diagnosis of so-called *ALSmimic* disorders [50]. Second, we could not test the diagnostic accuracy of the pulvinar volume in presymptomatic *C9orf72* mutation carriers to confirm that this is a very early developing endophenotype.

CONCLUSIONS

We identified anatomo-functional alterations of the pulvinar–cortical circuit in *ALSC9*+ patients. Pulvinar volume, according to the suggested cutpoint, could be a differential biomarker closely related to ALS and FTD driven by *C9orf72*. Furthermore, pulvinar subregions, due to their function as timekeepers for large-scale cortical networks [20], could play a crucial role in disease development and progression not only in the genetic phenotype but also in wild-type ALS.

AUTHOR CONTRIBUTIONS

Anna Nigri: Conceptualization; methodology; formal analysis; investigation; data curation; writing – original draft; project administration; validation. **Mario Stanziano:** Conceptualization; writing – original draft; validation; investigation; data curation. **Davide Fedeli:** Conceptualization; writing – original draft; data curation; methodology; software; visualization; validation; investigation. **Umberto Manera:** Data curation; investigation; writing – review and editing; formal analysis. **Stefania Ferraro:** Funding acquisition; writing – review and editing; resources. **Jean Paul Medina Carrion:** Methodology; software; formal analysis; writing – review and editing. **Sara Palermo:** Formal analysis; writing – review and editing; resources. **Laura Lequio:** Resources; writing – review

and editing. **Federica Denegri:** Resources; writing – review and editing. **Federica Agosta:** Funding acquisition; validation; formal analysis; writing – review and editing. **Edoardo Gioele Spinelli:** Formal analysis; validation; writing – review and editing. **Massimo Filippi:** Validation; writing – review and editing; formal analysis. **Marina Grisoli:** Validation; formal analysis; writing – review and editing. **Maria Consuelo Valentini:** Resources; funding acquisition; data curation. **Filippo De Mattei:** Data curation; writing – review and editing; resources. **Antonio Canosa:** Validation; formal analysis; writing – review and editing. **Andrea Calvo:** Validation; formal analysis; writing – review and editing. **Adriano Chiò:** Conceptualization; supervision; resources; data curation; funding acquisition; writing – review and editing. **Maria Grazia Bruzzone:** Conceptualization; funding acquisition; supervision; formal analysis; validation; writing – review and editing. **Cristina Moglia:** Conceptualization; writing – original draft; investigation; validation; formal analysis; data curation; supervision; resources; project administration.

ACKNOWLEDGMENTS

We thank the technicians (Francesco Primo, Roberto Agliata, Lucy Stefanelli, Rosalba Caruana, Nicola Mazzei, Manuela D'Ambrosio, Gianfranco Tagliente, Francesca Stancati) and radiologists (Giovanna Carrara, Maurizio Cogogni, Ivan Gomez Pavanello, Paola Sciortino, Fabrizio Venturi) of the Neuroradiology Unit, AOU Città della Salute e della Scienza and the GARR consortium for the high-performance infrastructure.

FUNDING INFORMATION

This work was in part supported by the Italian Ministry of Health (Ministero della Salute, Ricerca Sanitaria Finalizzata and Giovani Ricercatori, grant RF-2016-02362405, GR-2019-12371291, RRC), the European Commission's Health Seventh Framework Programme (FP7/2007–2013 under grant agreement 259867), the Italian Ministry of Education, University, and Research (Progetti di Ricerca di Rilevante Interesse Nazionale, grant 2017SNW5MB), and the Joint Programme–Neurodegenerative Disease Research (ALS-Care, Strength and Brain-Mend projects), granted by the Italian Ministry of Education, University, and Research. This study was performed under the Department of Excellence grant of the Italian Ministry of Education, University, and Research to the "Rita Levi Montalcini" Department of Neuroscience, University of Turin, Italy.

CONFLICT OF INTEREST STATEMENT

A.Ch. serves on scientific advisory boards for Mitsubishi Tanabe, Biogen, Roche, Denali Pharma, Cytokinetics, Lilly, and Amylyx Pharmaceuticals and has received a research grant from Biogen. None of the other authors has any conflict of interest to disclose.

DATA AVAILABILITY STATEMENT

Data will be available upon request by interested researchers. M.S. had full access to all of the data in the study and takes responsibility for the integrity of the data and the accuracy of the data analysis.

ETHICAL APPROVAL

Institutional review board approval was obtained by the Ethical Committee of the Azienda Ospedaliero-Universitaria Città della Salute of Turin (Protocol N.0021674–24/02/2022). Written informed consent was obtained from all patients in this study.

ORCID

Anna Nigri https://orcid.org/0000-0002-1197-5458
Umberto Manera https://orcid.org/0000-0002-9995-8133
Jean Paul Medina Carrion https://orcid.org/0000-0002-6450-0202
Massimo Filippi https://orcid.org/0000-0002-5485-0479
Andrea Calvo https://orcid.org/0000-0002-5122-7243
Cristina Moglia https://orcid.org/0000-0001-7377-7222

REFERENCES

1. Chiò A, Pagani M, Agosta F, Calvo A, Cistaro A, Filippi M. Neuroimaging in amyotrophic lateral sclerosis: insights into structural and functional changes. *Lancet Neurol*. 2014;13:1228-1240.
2. DeJesus-Hernandez M, Mackenzie IR, Boeve BF, et al. Expanded GGGGCC hexanucleotide repeat in noncoding region of C9ORF72 causes chromosome 9p-linked FTD and ALS. *Neuron*. 2011;72:245-256.
3. Majounie E, Renton AE, Mok K, et al. Frequency of the C9orf72 hexanucleotide repeat expansion in patients with amyotrophic lateral sclerosis and frontotemporal dementia: a cross-sectional study. *Lancet Neurol*. 2012;11:323-330.
4. Grassano M, Calvo A, Moglia C, et al. Systematic evaluation of genetic mutations in ALS: a population-based study. *J Neurol Neurosurg Psychiatry*. 2022;93:1190-1193.
5. Marogianni C, Rikos D, Provatas A, et al. The role of C9orf72 in neurodegenerative disorders: a systematic review, an updated meta-analysis, and the creation of an online database. *Neurobiol Aging*. 2019;84(238):e25-238.e34.
6. Trojsi F, Siciliano M, Femiano C, et al. Comparative analysis of C9Orf72 and sporadic disease in a large multicenter ALS population: the effect of male sex on survival of C9Orf72 positive patients. *Front Neurosci*. 2019;13:1-10.
7. Irwin DJ, McMillan CT, Brettschneider J, et al. Cognitive decline and reduced survival in C9orf72 expansion frontotemporal degeneration and amyotrophic lateral sclerosis. *J Neurol Neurosurg Psychiatry*. 2013;84:163-169.
8. Byrne S, Elamin M, Bede P, et al. Cognitive and clinical characteristics of patients with amyotrophic lateral sclerosis carrying a C9orf72 repeat expansion: a population-based cohort study. *Lancet Neurol*. 2012;11:232-240.
9. Millecamps S, Boillée S, Le Ber I, et al. Phenotype difference between ALS patients with expanded repeats in C9ORF72 and patients with mutations in other ALS-related genes. *J Med Genet*. 2012;49:258-263.
10. Chipika RH, Finegan E, Li Hi Shing S, et al. "Switchboard" malfunction in motor neuron diseases: selective pathology of thalamic nuclei in amyotrophic lateral sclerosis and primary lateral sclerosis. *NeuroImage Clin*. 2020;27:102300.
11. Querin G, Biferi MG, Pradat PF. Biomarkers for C9orf7-ALS in symptomatic and pre-symptomatic patients: state-of-the-art in the new era of clinical trials. *J Neuromuscul Dis*. 2022;9:25-37.
12. Spinelli EG, Ghirelli A, Basaia S, et al. Structural MRI signatures in genetic presentations of the frontotemporal dementia/motor neuron disease Spectrum. *Neurology*. 2021;97:E1594-E1607.

13. Bocchetta M, Todd EG, Peakman G, et al. Differential early subcortical involvement in genetic FTD within the GENFI cohort. *NeuroImage Clin*. 2021;30:8-11.
14. Bocchetta M, Iglesias JE, Neason M, Cash DM, Warren JD, Rohrer JD. Thalamic nuclei in frontotemporal dementia: mediodorsal nucleus involvement is universal but pulvinar atrophy is unique to C9orf72. *Hum Brain Mapp*. 2020;41:1006-1016.
15. Bocchetta M, Todd EG, Tse NY, et al. Thalamic and cerebellar regional involvement across the ALS–FTD Spectrum and the effect of C9orf72. *Brain Sci*. 2022;12:1-16.
16. McKenna MC, Li Hi Shing S, Murad A, et al. Focal thalamus pathology in frontotemporal dementia: phenotype-associated thalamic profiles. *J Neurol Sci*. 2022;436:120221.
17. Lee SE, Khazenzon AM, Trujillo AJ, et al. Altered network connectivity in frontotemporal dementia with C9orf72 hexanucleotide repeat expansion. *Brain*. 2014;137:3047-3060.
18. Saalmann YB, Pinsk MA, Wang L, et al. The pulvinar regulates information transmission between cortical areas based on attention demands. *Science (80-)*. 2012;337:753-756.
19. Barron DS, Eickhoff SB, Clos M, Fox PT. Human pulvinar functional organization and connectivity. *Hum Brain Mapp*. 2015;36:2417-2431.
20. Fiebelkorn IC, Kastner S. The puzzling pulvinar. *Neuron*. 2019;101:201-203.
21. Guedj C, Vuilleumier P. Functional connectivity fingerprints of the human pulvinar: decoding its role in cognition. *Neuroimage*. 2020;221:117162.
22. Jaramillo J, Mejias JF, Wang XJ. Engagement of Pulvino-cortical feedforward and feedback pathways in cognitive computations. *Neuron*. 2019;101:321-336.e9.
23. Brooks BR, Miller RG, Swash M, Munsat TL. El Escorial revisited: revised criteria for the diagnosis of amyotrophic lateral sclerosis. *Amyotroph Lateral Scler*. 2000;1:293-299.
24. Nigri A, Umberto M, Stanziano M, et al. C9orf72 ALS mutation carriers show extensive cortical and subcortical damage compared to matched wild-type ALS patients. *NeuroImage Clin*. 2023;38:103400. doi:10.1016/j.nicl.2023.103400
25. Stanziano M, Fedeli D, Manera U, et al. Resting-state fMRI functional connectome of C9orf72 mutation status. *Ann Clin Transl Neurol*. 2024;1-12. doi:10.1002/acn3.51989
26. Balendra R, Jones A, Jivraj N, et al. Estimating clinical stage of amyotrophic lateral sclerosis from the ALS functional rating scale. *Amyotroph Lateral Scler Front Degener*. 2014;15:279-284.
27. Fischl B. FreeSurfer. *Neuroimage*. 2012;62:774-781.
28. Iglesias JE, Insausti R, Lerma-Usabiaga G, et al. A probabilistic atlas of the human thalamic nuclei combining ex vivo MRI and histology. *Neuroimage*. 2018;183:314-326.
29. Whitfield-Gabrieli S, Nieto-Castanon A. Conn: a functional connectivity toolbox for correlated and anticorrelated brain networks. *Brain Connect*. 2012;2:125-141.
30. Ashburner J, Friston KJ. Unified segmentation. *Neuroimage*. 2005;26:839-851.
31. Chai XJ, Castañán AN, Öngür D, et al. Anticorrelations in resting state networks without global signal regression. *Neuroimage*. 2012;59:1420-1428.
32. Nieto-Castanon A. *Handbook of Functional Connectivity Magnetic Resonance Imaging Methods in CONN*. Hilbert Press; 2020.
33. Virtanen P, Gommers R, Oliphant TE, et al. SciPy 1.0: fundamental algorithms for scientific computing in python. *Nat Methods*. 2020;17:261-272.
34. Seabold S, Perktold J. Statsmodels: Econometric and statistical modeling with python. In: *Proceedings of the 9th Python in Science Conference*. 2010, pp. 10–25080.
35. Thiele C, Thiele MC. Package 'cutpointr'.
36. Schönecker S, Neuhofer C, Otto M, et al. Atrophy in the thalamus but not cerebellum is specific for C9orf72 FTD and ALS patients – an atlas-based volumetric MRI study. *Front Aging Neurosci*. 2018;10:1-11.
37. Agosta F, Ferraro PM, Riva N, et al. Structural and functional brain signatures of C9orf72 in motor neuron disease. *Neurobiol Aging*. 2017;57:206-219.
38. Byne W, Hazlett EA, Buchsbaum MS, Kemether E. The thalamus and schizophrenia: current status of research. *Acta Neuropathol*. 2009;117:347-368.
39. Kemether EM, Buchsbaum MS, Byne W, et al. Magnetic resonance imaging of mediodorsal, pulvinar, and centromedian nuclei of the thalamus in patients with schizophrenia. *Arch Gen Psychiatry*. 2003;60:983-991.
40. Loewe K, Machts J, Kaufmann J, et al. Widespread temporo-occipital lobe dysfunction in amyotrophic lateral sclerosis. *Sci Rep*. 2017;7:1-9.
41. Douand G, Filippini N, Knight S, et al. Integration of structural and functional magnetic resonance imaging in amyotrophic lateral sclerosis. *Brain*. 2011;134:3470-3479.
42. Zhang J, Ji B, Hu J, et al. Aberrant interhemispheric homotopic functional and structural connectivity in amyotrophic lateral sclerosis. *J Neurol Neurosurg Psychiatry*. 2017;88:374-380.
43. Zhou F, Gong H, Li F, et al. Altered motor network functional connectivity in amyotrophic lateral sclerosis : a resting-state functional magnetic resonance imaging study. *Neuroreport*. 2013;24:657-662.
44. Menke RAL, Proudfoot M, Talbot K, et al. The two-year progression of structural and functional cerebral MRI in amyotrophic lateral sclerosis. *NeuroImage Clin*. 2018;17:953-961.
45. Crockford C, Newton J, Lonergan K, et al. ALS-specific cognitive and behavior changes associated with advancing disease stage in ALS. *Neurology*. 2018;91:E1370-E1380.
46. Bede P, Siah WF, McKenna MC, et al. Consideration of C9orf72 – associated ALS-FTD as a neurodevel opmental disorder: insights from neuroimaging. *J Neurol Neurosurg Psychiatry*. 2020;91:1138.
47. Shoukry RS, Waugh R, Bartlett D, Raitcheva D, Floeter MK. Longitudinal changes in resting state networks in early presymptomatic carriers of C9orf72 expansions. *NeuroImage Clin*. 2020;28:102354.
48. Rittman T, Borchert R, Jones S, et al. Functional network resilience to pathology in presymptomatic genetic frontotemporal dementia. *Neurobiol Aging*. 2019;77:169-177.
49. Tsvetanov KA, Gazzina S, Jones PS, et al. Brain functional network integrity sustains cognitive function despite atrophy in presymptomatic genetic frontotemporal dementia. *Alzheimers Dement*. 2021;17:500-514.
50. Agosta F, Spinelli EG, Filippi M. Neuroimaging in amyotrophic lateral sclerosis: current and emerging uses. *Expert Rev Neurother*. 2018;18:395-406.

SUPPORTING INFORMATION

Additional supporting information can be found online in the Supporting Information section at the end of this article.

How to cite this article: Nigri A, Stanziano M, Fedeli D, et al. Distinct neural signatures of pulvinar in *C9orf72* amyotrophic lateral sclerosis mutation carriers and noncarriers. *Eur J Neurol*. 2024;00:e16266. doi:10.1111/ene.16266